Available online at www.sciencedirect.com
ScienceDirect
Coastal Engineering 55 (2008) 319–332
Coastal Engineering
An International Journal for Coastal, Harbour and Offshore Engineers
www.elsevier.com/locate/coastaleng

The effect of a topographic high on the morphological stability of a two-inlet bay system

J. van de Kreeke [a,*], R.L. Brouwer [b], T.J. Zitman [b], H.M. Schuttelaars [c]

[a] Rosenstiel School of Marine and Atmospheric Science, University of Miami, 4600 Rickenbacker Causeway, Miami, Fl, 33149 USA
[b] Section of Hydraulic Engineering, Delft University of Technology, P.O. Box 5048, 2600 GA, Delft, The Netherlands
[c] Institute of Applied Mathematics, Delft University of Technology, Mekelweg 4, 2600 GA, Delft, The Netherlands

Received 6 March 2007; received in revised form 7 October 2007; accepted 23 November 2007
Available online 10 January 2008

Abstract

The cross-sectional stability of two tidal inlets connecting the same back-barrier lagoon to the ocean is investigated. The condition for equilibrium is the cross-sectional area tidal prism relationship. In an earlier study [Van de Kreeke, J., 1990. Can multiple inlets be stable? Estuarine, Coastal and Shelf Science 30: 261–273.], using the same equilibrium condition, it was concluded that where two inlets connect the same basin to the ocean ultimately one inlet will close. One of the major assumptions in that study was that the water level in the basin fluctuated uniformly. In hindsight this assumption might be too restrictive. For example, in the Wadden Sea the back barrier lagoon consists of a series of basins, rather than one single basin, separated by topographic highs. These topographic highs limit but do not exclude the exchange of water between the sub-basins. For this reason in the present study, a topographic high in the form of a weir was added, separating the back-barrier lagoon in two sub-basins. The water level in the sub-basins, rather than in the back-barrier as a whole, is assumed to fluctuate uniformly. For this schematization the hydrodynamic equations are solved using a finite difference method. The results, together with the equilibrium condition, yield the equilibrium flow curve for each of the inlets. The intersections of the two equilibrium flow curves represent combinations of cross-sectional areas for which both inlets are in equilibrium. The stability of the equilibriums was investigated using a non-linear stability analysis resulting in a flow diagram. Calculations were carried out for different inlet and weir characteristics. Sinussoidal tides were the same for both inlets. The results show that for relatively large wetted cross-sectional areas over the topographic high, approaching the situation of a single basin, there are no combinations of inlet cross-sectional areas for which both inlets are in a stable equilibrium. This supports the conclusion in the earlier study. For relatively small wetted cross-sectional areas over the topographic high there is one set of stable equilibriums. In that case the two-inlet bay system approaches that of two single-inlet bay systems.

Keywords: tidal inlet; morphology; morphodynamic equilibrium; stability analysis; Wadden Sea

1. Introduction

A considerable part of the world's coasts consists of barrier islands. These islands are separated by tidal inlets, relatively short and narrow channels that connect the back-barrier lagoons to the ocean. Restricting attention to inlets that are scoured in loose-granular material, the cross-sectional area of these inlet channels takes on a value where on averaged annual basis the sand transport into the inlet equals the sand transport out of the inlet. The actual cross-sectional area oscillates about this equilibrium value. When the oscillations become too large, the inlet cross-section could become unstable and the inlet might close.

It was Escoffier (1940) who first proposed a method to determine the equilibrium and stability of a tidal inlet. He reasoned that the equilibrium values of the inlet cross-sectional areas are the intersections of the closure curve (the relationship of the amplitude of the inlet velocity and the inlet cross-sectional area) and an empirical quantity, the equilibrium velocity. In general there will be two intersections, one representing a stable and the other an unstable equilibrium.

* Corresponding author.
E-mail address: jvandekreeke@rsmas.miami.edu (J. van de Kreeke).

0378-3839/$ - see front matter © 2007 Elsevier B.V. All rights reserved.
doi:10.1016/j.coastaleng.2007.11.010

Closure curves are calculated by solving the governing hydrodynamic equations. In many of the earlier studies, when calculating closure curves the continuity equation was simplified by assuming a uniformly fluctuating lagoon level. This allowed analytical or semi-analytical solutions (Brown, 1928; Keulegan, 1951; Van de Kreeke, 1967; Mehta and Ozsoy, 1978; Walton and Escoffier, 1981; DiLorenzo, 1988). However, it is pointed out this assumption is not essential to the stability concept as proposed by Escoffier. Solving the equations without making the simplifying assumption of a uniformly fluctuating lagoon level can be relatively easily accomplished using numerical methods.

As will be discussed in some detail in Section 2.2, the equilibrium velocity is related to the cross-sectional area-tidal prism relationship for inlets at equilibrium. In general the equilibrium velocity is a weak function of the inlet cross-sectional area. Only when the relation between cross-sectional area and tidal prism is linear is the equilibrium velocity constant; a simplifying assumption Escoffier (1940) made in presenting his stability concept. The cross-sectional area tidal prism relationship for inlets at equilibrium originally was purely empirical (e.g. O'Brien, 1931; Jarrett, 1976; Bruun and Gerritsen, 1960). Only recently this relationship and therewith the equilibrium velocity was given a physical footing (Van de Kreeke, 1998, 2004; Kraus, 1998; Suprijo and Mano, 2004).

Even though Escoffier presented his stability concept in 1940, it was not until the early seventies that engineers started to use it (O'Brien and Dean, 1972). This might have partly to do with some of the practical problems encountered when applying the concept to actual inlets. A discussion of these problems and possible solutions can be found in Van de Kreeke (2004) and Walton (2004). Even today, in spite of recent advances in our understanding of sediment transport by waves and currents, Escoffier's stability concept is still the method of choice (Van de Kreeke, 2004).

Most studies mentioned so far concentrated on single-inlet bay systems, even though the majority of back-barrier lagoons are connected to the ocean by more than one inlet. An exception is the study by Van de Kreeke (1990), who specifically addressed the stability of multiple-inlet bay systems thereby taking into account the interaction of the inlets. In this study it was concluded that, where more than one inlet connects a tidal bay to the ocean, inlets can not be in a stable equilibrium simultaneously. Ultimately only one inlet will remain open and the others will close. In arriving at

Fig. 1. Wadden Sea; Texel and Vlie basin with topographic high (white lines).

this conclusion a number of assumptions were made with regards to morphometry and boundary conditions. The tidal inlet system was schematized to a basin and two prismatic inlet channels. Inlet channels were assumed to be relatively long making entrance and exit energy losses small compared to frictional losses. Furthermore in describing the inlet dynamics inertia was neglected. The basin dimensions were assumed to be small compared to tidal wave length, justifying the assumption of a uniformly fluctuating water level (pumping mode). The ocean tides off the two inlets were assumed to be the same and simple harmonic. This simplified model was believed to represent sufficiently the relevant hydrodynamic processes affecting stability.

In hindsight, some of the assumptions in Van de Kreeke (1990) might be too restrictive as there are examples of inlets connecting the same bay to the ocean that have been in a stable equilibrium for centuries. Examples are the inlets of the Venice Lagoon (Tambroni and Seminara, 2006), the Rio Formosa (Salles et al, 2005) and the Wadden Sea (Louters and Gerritsen, 1994). A closer look at, for example, the Wadden Sea system shows that the back barrier lagoon consists of a series of basins as opposed to a single basin (Fig. 1). These basins are separated by topographic highs. The topographic highs are roughly located at places where the tides entering the inlets meet. They act as semi-permeable barriers that allow a certain degree of exchange of water between the two sub-basins. Hence the assumption of a uniformly fluctuating bay level might be valid for the sub-basins but not for the basin as a whole.

The main aim of the present study is to extend the model in Van de Kreeke (1990) by including the effects of topographic highs and to use this model to study the existence and stability of two-inlet bay systems. Hence the basin is divided in two sub-basins by a topographic high. Based on observations in the Wadden Sea the topographic high extends across the bay and has a uniform elevation somewhat below the mean water level to allow for exchange between the sub-basins. The schematization of the inlet system without a topographic high is the same as used in the earlier study and is presented in Fig. 2a. The schematization with topographic high is presented in Fig. 2b. In addition to including a topographic high, inertia has been added to the dynamic equations for the inlet flow. Forcing is by identical sinusoidal tides off the inlets.

The aforementioned relatively simple schematization and model has the advantage that it can be used as a diagnostic tool to gain further insight into the mechanisms causing or hampering stability of multiple inlet systems. Unfortunately the addition of a topographic high and the inclusion of inertia in the dynamic equations for the inlet flow do not allow an analytical solution to the stability problem as used in Van de Kreeke (1990). Instead, recourse has to be taken to a numerical approach.

2. Equilibrium and stability

2.1. General

The focus of this study is on equilibriums whereby both inlets are open (as opposed to one open and one closed inlet). In determining the equilibrium value of the cross-sectional area of an inlet, the basic premise is that on an annual averaged basis the volume of sand transported into the inlet is constant, its value depending on the littoral drift. This influx of sand is balanced by the transport of sand out of the inlet by the ebb tidal currents. In principle when the flow field is known, the sand transported out of the inlet can be calculated using relationships between velocity and transport. However, in using this procedure there are several difficulties in arriving at reliable estimates of the transport. These include:

- Sand transport, in addition to tidal flow, is a function of waves. The relation between sediment transport and velocity field induced by tide and waves is not well known.
- Sand transport is largely in the form of suspended load; accurate modeling is difficult as the suspended transport, in addition to the velocity field in the inlet, depends on the velocity field and sediment transport processes in the back-barrier lagoon including erosion and deposition.
- Residual (tidally averaged) transport depends on non-linearities in the flow which requires a highly accurate hydrodynamic model.

In view of these difficulties, in this study a more pragmatic approach is taken. Instead of calculating sand transport, the well-known empirical relationship between inlet cross-sectional area and ebb tidal prism for inlets at equilibrium is used. The approach is described in detail in Sections 2.2 and 2.3.

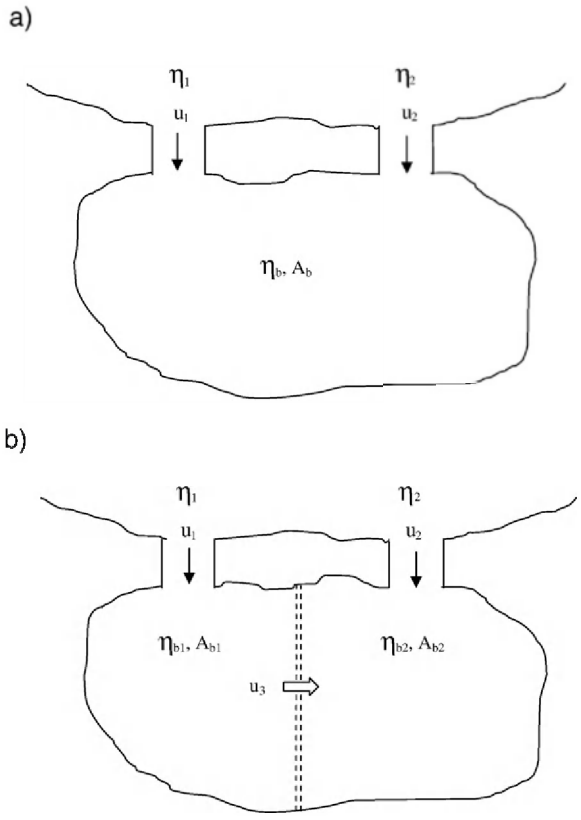

Fig. 2. Schematization of two-inlet bay system (a) without and (b) with topographic high.

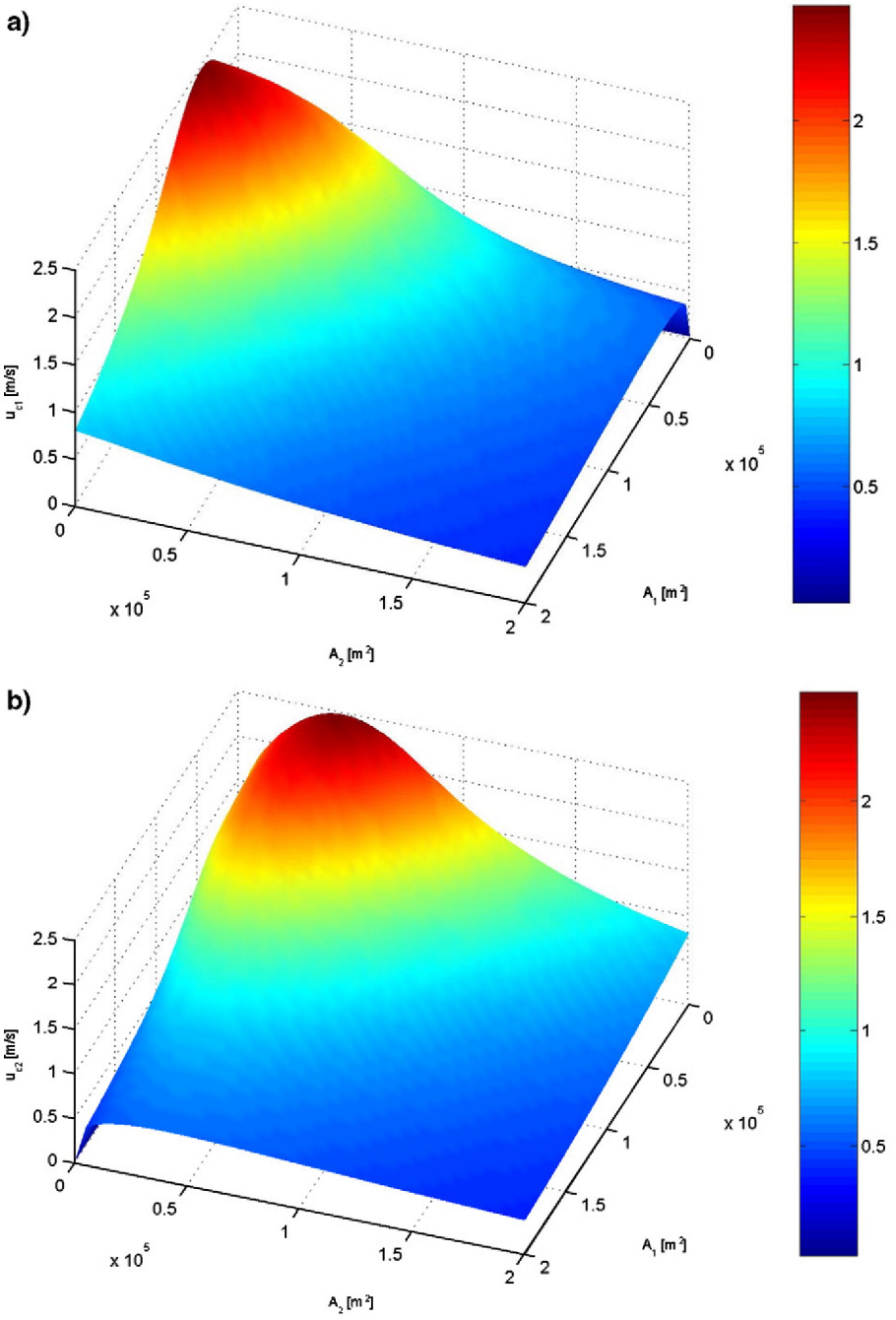

Fig. 3. Closure surfaces for (a) inlet 1 and (b) inlet 2.

2.2. Equilibrium

For inlets at equilibrium the following relationship between cross-sectional area and tidal prism exists

$$A = CP^q \tag{1}$$

where A is cross-sectional area, P is ebb tidal prism. A and P are considered annually averaged values. C and q are constants that among other things are functions of volume of littoral drift and grain size. As stated in the Introduction, Eq. (1) was initially introduced as an empirical relationship and only recently attempts have been made to give this relationship a physical footing.

For purposes of this study, it is convenient to express the equilibrium condition, Eq. (1), in terms of velocity. For this the characteristic velocity $\hat{u}_c$ is introduced. Approximating the ebb tidal velocity by a half sine with amplitude $\hat{u}_c$ and a period T equal to twice the duration of the ebb

$$\hat{u}_{c_i} = \frac{\pi P_i}{A_i T} \quad i = 1, 2 \tag{2}$$

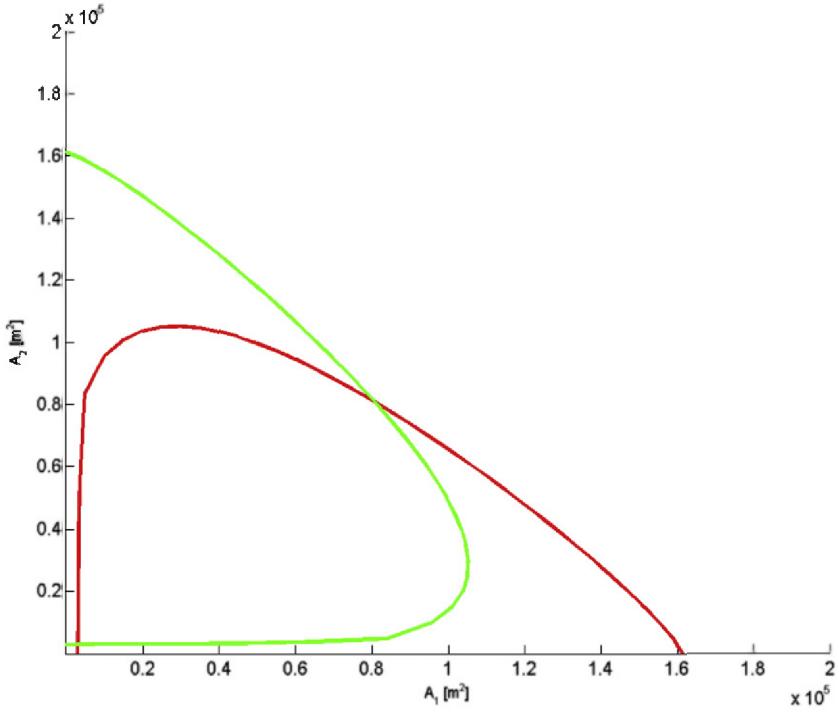

Fig. 4. Equilibrium flow curves for inlets 1 (red) and 2 (green). (For interpretation of the references to colour in this figure legend, the reader is referred to the web version of this article.)

Subscripts refer to inlets 1 and 2. Because the tidal prism is a function of both A_1 and A_2, the characteristic velocity $\hat{u}_{c_i}$ is a function of A_1 and A_2,

$$\hat{u}_{c_i} = f(A_1, A_2) \quad i = 1, 2 \tag{3}$$

Eq. (3) represents a surface referred to as the closure surface. A typical shape of the closure surface for the inlets is presented in Fig. 3a and b. Referring to the closure surface for inlet 1 in Fig. 3a, for constant A_2 values of $\hat{u}_{c_1}$ increase with increasing values of A_1, reaching a maximum and subsequently decreases gradually to a zero value for large A_1. For constant values of A_1, $\hat{u}_{c_1}$ monotonically decreases with increasing values of A_2. Using Fig. 3b, a similar description holds for the closure surface of inlet 2.

It follows from Eqs. (1) and (2) that for inlets that are in equilibrium

$$\hat{u}_{c_i} = \hat{u}_{\mathrm{eq}_i} = \left(\pi / \left(TC^{1/q}\right)\right) A_i^{[(1/q)-1]} \quad i = 1, 2 \tag{4}$$

Values of q, C and T are assumed to be the same for both inlets. For the Dutch Wadden Sea and using the metric system to a good approximation $q=1$, $C=6.8\ 10^{-5}$ and $T=44{,}712$ s (Van de Kreeke, 1998). With $q=1$, it follows from Eq. (4) that $\hat{u}_{\mathrm{eq}_i}$ is independent of A_i. Therefore, for identical C and T, $\hat{u}_{\mathrm{eq}}$ is the same for both inlets and equal to $\hat{u}_{\mathrm{eq}}=1.03$ m/s. $\hat{u}_{\mathrm{eq}}$ will be referred to as the equilibrium velocity.

To determine the values of (A_1, A_2) for which both inlets are in equilibrium, use is made of the so-named equilibrium flow curves. The equilibrium flow curve of inlet 1 represents the locus of the values (A_1, A_2) for which for that inlet $\hat{u}_{c_i} = \hat{u}_{eq}$ and similar for inlet 2. Geometrically, the equilibrium flow curve for inlet 1 is the intersection of the plane $\hat{u}_{c_1} = \hat{u}_{eq}$ with the closure surface of inlet 1 and similar for inlet 2. A typical example of equilibrium flow curves for a two-inlet bay system is presented in Fig. 4. The intersections of the equilibrium flow curves represent combinations of (A_1, A_2) for which both inlets are in equilibrium.

2.3. Stability

An inlet is in a stable equilibrium, when after having been perturbed, it will return to that equilibrium. In the case of the two-inlet bay system the stability of the equilibrium can be determined by visual inspection of the configuration of the equilibrium flow curves in the neighborhood of the equilibrium. The criterion is that when $\hat{u}_{c_i} > \hat{u}_{\mathrm{eq}}$ the inlet cross-sectional area will increase and when $\hat{u}_{c_i} > \hat{u}_{\mathrm{eq}}$ the cross-sectional area will decrease. An example of determining the stability in this fashion can be found in Jain et al. (2004).

A more unambiguous approach would be to apply a linear stability analysis. However, the results of this analysis would be limited to the (A_1, A_2) space in close proximity of the equilibrium. Instead, in this study a flow diagram is used. A flow diagram consists of the equilibrium flow curves together with a vector plot. The vectors represent the adaptation, or more precisely the rate of change of the cross-sectional areas, $\mathrm{d}A_1/\mathrm{d}t$ and $\mathrm{d}A_2/\mathrm{d}t$, after both cross-sections have been removed from equilibrium. The vectors are defined as

$$\frac{d\vec{A}}{dt} = \frac{dA_1}{dt}\vec{e}_1 + \frac{dA_2}{dt}\vec{e}_2 \tag{5}$$

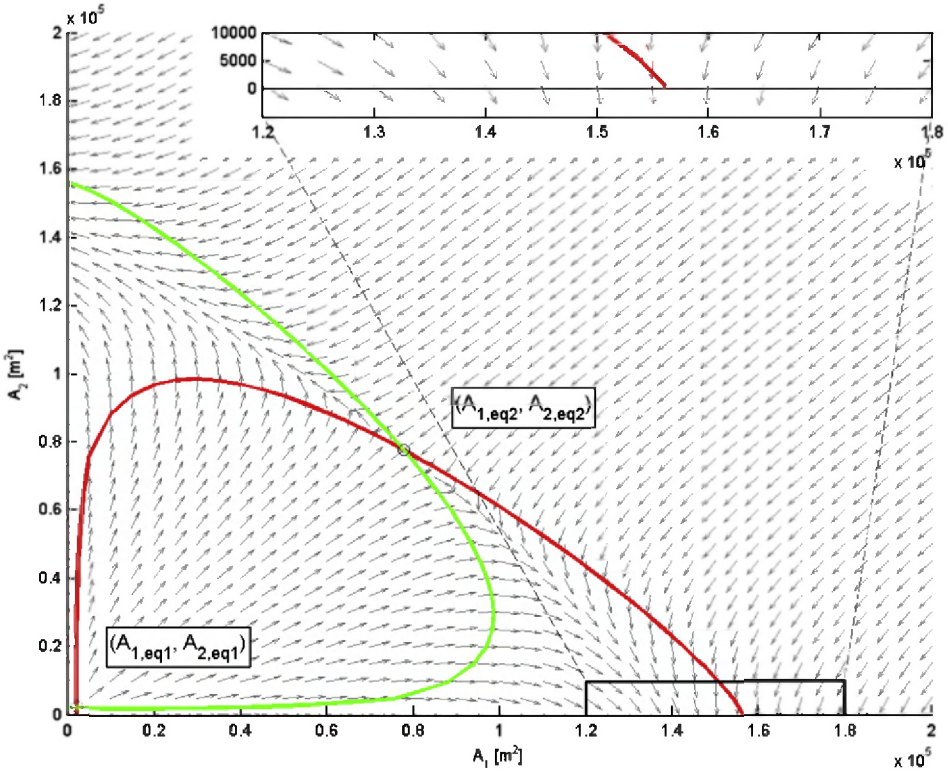

Fig. 5. Flow diagram for a two-inlet bay system without topographic high. For parameter values see Table 1. Equilibrium flow curves for inlets 1 (red) and 2 (green). (For interpretation of the references to colour in this figure legend, the reader is referred to the web version of this article.)

where $\vec{e}_1$ and $\vec{e}_2$ are the unit vectors in respectively the direction of the A_1 axis and A_2 axis. The rate of change of the cross-sectional areas of the inlets can be related to the characteristic velocity as follows. The value of $q=1$ for the Wadden Sea inlets corresponds to an annually averaged transport of sand during the ebb period (export) that is proportional to a power n of the characteristic velocity (Van de Kreeke, 2004),

$$\mathrm{TR}_i = k\hat{u}_{c_i}^n \tag{6}$$

TR_i is a volume transport and k is a dimensional constant, its value dependent on sand characteristics. n is a constant with a value between 3 and 5. On an annually averaged basis the volume of sand entering the inlet, M, is taken equal to a fraction of the volume of littoral drift. Therefore, when an inlet is at equilibrium,

$$\mathrm{TR}_i = M = k\hat{u}_{\mathrm{eq}}^n \tag{7}$$

M is assumed to be independent of the cross-sectional area of the inlet. Furthermore, assuming no exchange of sand between inlet channel and back-barrier lagoon, the rate of change of cross-sectional area A_i is

$$L_i\frac{dA_i}{dt} = k\hat{u}_i^n - k\hat{u}_{eq}^n \quad A_i>0 \tag{8}$$

L_i is the length of the inlet channel. The assumption here is that the entire length of the channel is involved in the shoaling process. Applying the foregoing to a two-inlet bay system and assuming M and therefore k (Van de Kreeke, 2004) to be the same for both inlets,

$$\frac{dA_i}{dt} = \frac{M}{L_i}\left[\left(\frac{\hat{u}_{c_i}}{\hat{u}_{\mathrm{eq}}}\right)^n - 1\right] \quad i=1,2 \quad A_i>0 \tag{9}$$

Making use of Eqs. (5) and (9) an example of a flow diagram is presented in Fig. 5. For the parameter values used to construct the diagram reference is made to Table 1. (note: the equilibrium flow curves in this figure are the same as those presented in Fig. 4.) Because here the direction rather than the magnitude of the vector is of interest, vectors dA_i/dt in the flow diagram are given a unit length. There are two intersections of the equilibrium flow curves and therefore there are two equilibriums for which both inlets are open. Directions of the vectors in the vicinity of the equilibriums show whether after a perturbation the system will respond by returning to the equilibrium or moving further away from it. For this the flow diagrams in the vicinity of the equilibriums are enlarged in Fig. 6. From the direction of the vectors it follows that both equilibriums are unstable.

Table 1
Parameter values used in calculating Figs. 3, 4, 5 and 6

$L_1=L_2=5000$ m	$\eta_1=\eta_2=0.75\cos\sigma t$
$F_1=F_2=0.004$	$\sigma=2\pi/44{,}712$ s^{-1}
$\gamma_1=\gamma_2=0.065$	
$A_b=14\cdot10^8$ m^2	
$\hat{u}_{\mathrm{eq}}=1.03$ m/s	

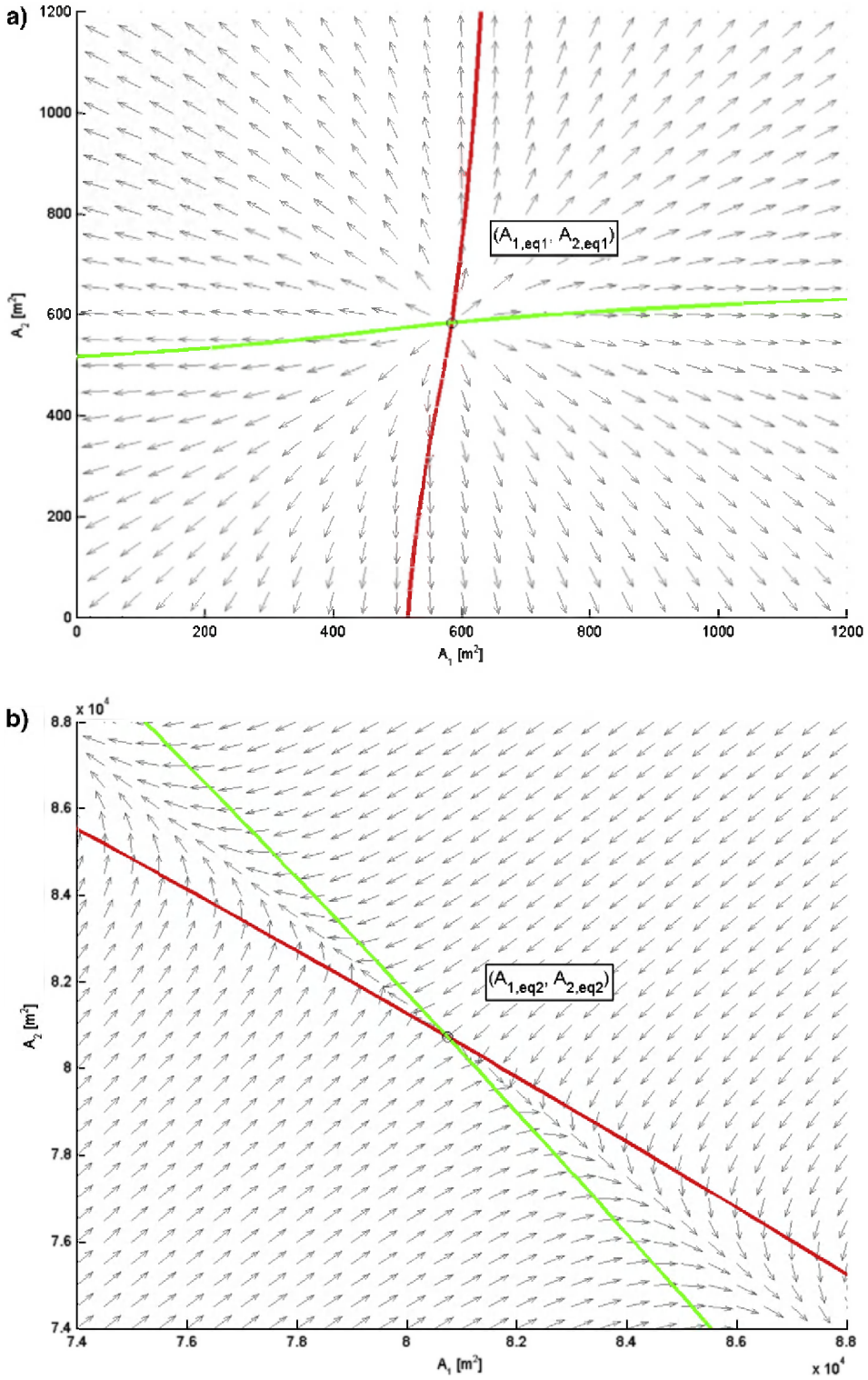

Fig. 6. Flow diagram for a two-inlet bay system without topographic high (a) close-up around the equilibrium ($A_{1,eq1}$, $A_{2,eq1}$) in Fig. 5 and (b) close-up around the equilibrium ($A_{1,eq2}$, $A_{2,eq2}$) in Fig. 5. Equilibrium flow curves for inlets 1 (red) and 2 (green). (For interpretation of the references to colour in this figure legend, the reader is referred to the web version of this article.)

For the interpretation of the vectors near the axis of the flow diagram it should be realized that for $A_i=0$ there exists a discontinuity in the value of dA_i/dt. In the neighbourhood of $A_i=0$, $\hat{u}_{c_i}$ is a monotonously increasing function of A_i (Van de Kreeke, 2004). With $\hat{u}_{c_i}<\hat{u}_{eq}$ it then follows from Eq. (9) that dA_i/dt is negative with a magnitude that monotonously increases with decreasing value of A_i. The cross-sectional area decreases faster as A_i becomes smaller, which from a physics point of view seems reasonable. Furthermore from Eq. (9) when $A_i \rightarrow 0$ the rate of change of dA_i/dt approaches a constant value $dA_i/dt=-M/L_i$. On

the other hand for $A_i=0$, $dA_i/dt=0$. At first sight this discontinuity in dA_i/dt might seem strange but there is a simple explanation by comparing with the velocity of a falling stone. The velocity of the falling stone increases to reach a maximum just before reaching bottom. When touching bottom the velocity abruptly goes to zero.

The discontinuity in dA_i/dt for values of A_i approaching zero leads to some peculiarities in the flow diagram near the axis. In particular, vectors do not point at the intercept of equilibrium flow curve and axis. To further explain this an enlarged figure of the area in the neighbourhood of the intercept of the equilibrium flow curve for Inlet 1 and the A_1 axis is presented as an inset in Fig. 5. Near this intercept, inlet 2 is relatively small and it is closing rapidly. This process ends abruptly as soon as inlet 2 is closed. Simultaneously, inlet 1 evolves asymptotically and at a far smaller rate towards its equilibrium. This is reflected by the direction of the vectors in the figure. Their vertical components (dA_2/dt) are much larger than their horizontal ones (dA_1/dt). However, these horizontal components do point towards the equilibrium flow curve, indicating that the intercept corresponds to a stable equilibrium for inlet 1 when inlet 2 is closed. Although not shown in the figure, a similar close look at the other intercept of the equilibrium flow curve for inlet 1 with the A_1 axis reveals that horizontal components of nearby vectors point away from that intercept. This corresponds to an unstable equilibrium for inlet 1 when inlet 2 is closed. Hence, in the limiting case where $A_2 \rightarrow 0$, our model converges to the type of behaviour that is expected for a single inlet system: one stable and one unstable equilibrium, in conformity with the theory of Escoffier (1940).

3. Numerical experiments

In this section results of numerical experiments to determine the equilibrium and stability of two-inlet bay systems are summarized. Details of the computations can be found in Brouwer (2006). A distinction is made between two-inlet bay systems with and without topographic highs. Calculations are carried out with tide conditions and inlet and lagoon dimensions that are typical for the western Wadden Sea, i.e. inlet lengths 1–5 10^3 m, lagoon surface areas 4–14 10^8 m^2. The amplitudes and phases of the semi-diurnal sinusoidal tides off the inlets are the same. The value of the amplitudes used in the calculations is 0.75 m.

3.1. Two-inlet bay system without topographic high

3.1.1. Governing equations

For the schematization of the two-inlet bay system without topographic high reference is made to Fig. 2a. Prismatic inlet channels are assumed. The equations describing the water motion are the continuity equation,

$$A_b \frac{d\eta_b}{dt} = u_1 A_1 + u_2 A_2 \tag{10}$$

and for each inlet a one-dimensional momentum balance,

$$\frac{R_1}{F_1}\frac{du_1}{dt} + |u_1|u_1 = K_1(\eta_1 - \eta_b) \tag{11}$$

$$\frac{R_2}{F_2}\frac{du_2}{dt} + |u_2|u_2 = K_2(\eta_2 - \eta_b) \tag{12}$$

with

$$\eta_1 = \eta_2 = \hat{\eta}_0 \cos\sigma t \tag{13}$$

and

$$K_i = \frac{gR_i}{F_i L_i} \quad i = 1,2 \tag{14}$$

In these equations, A_b is bay surface area, η_b is bay tide, σ is tidal frequency, t is time and g is the gravitational constant. For inlet i, the ocean tide is denoted by η_i and u_i is the cross-sectionally averaged inlet velocity, A_i is the cross-sectional area of the inlet, L_i its length, R_i the hydraulic radius and F_i is a dimensionless friction factor. K_i is a coefficient of repletion (Keulegan, 1951). In deriving the equations the bay surface area is assumed to fluctuate uniformly, i.e. the water surface in the bay remains horizontal at all times. The inlet channels of the Dutch Wadden Sea are short compared to the length of the tidal wave, so that gradients of the cross-sectional averaged velocity in the direction of the channel axis can be neglected. However, channels are long enough for friction losses to dominate over entrance and exit losses. The inlet channels are relatively deep and as a result tidal variations in water level can be neglected.

To relate the hydraulic radius to the cross-sectional area, the cross-sections are assumed to remain geometrically similar i.e. the ratio of all corresponding lengths for two cross-sections remain the same. This allows writing

$$R_i = \gamma_i \sqrt{A_i} \quad i = 1,2 \tag{15}$$

where γ_i is a factor that depends on the shape of the cross-section. Substituting this expression in Eq. (14) results in the following expression for K_i

$$K_i = c_i \sqrt{A_i} \quad i = 1,2 \tag{16}$$

with

$$c_i = \frac{g\gamma_i}{F_i L_i} \quad i = 1,2 \tag{17}$$

3.1.2. Results

Typical results of the computations are presented in Figs. 3, 4 and 5. Parameter values used in the computations are presented in Table 1. The cross-sectional areas of the inlet channels are assumed to have a triangular shape with side slopes making an angle of 1° with the horizontal. Fig. 3a and b show the closure surfaces of inlets 1 and 2. Referring to Fig. 3a, for constant values of A_2 and increasing values of A_1, $\hat{u}_{c_1}$ increases to reach a maximum and after that gradually decrease. Values of $\hat{u}_{c_1}$ decrease for increasing values of A_2. A similar description holds for the closure surface of inlet 2 in Fig. 3b. Fig. 4 shows the equilibrium flow curves. The two intersections of the equilibrium flow curves represent combinations of (A_1, A_2) for which both inlets are in equilibrium. Plotting the

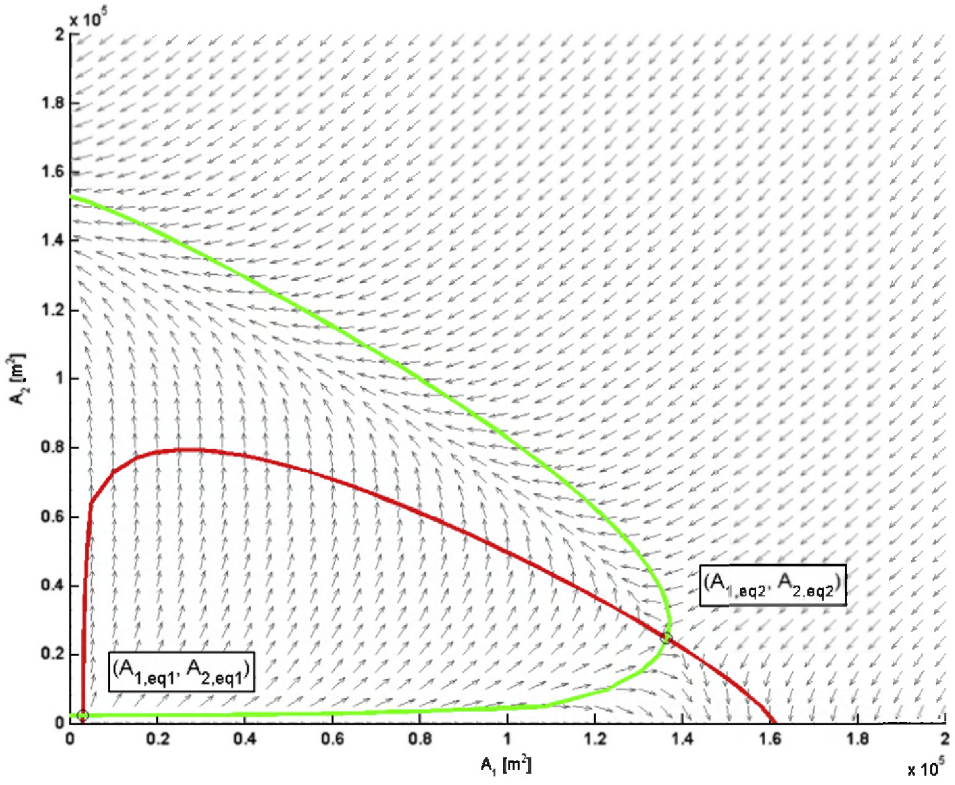

Fig. 7. Flow diagram for a two-inlet bay system without topographic high. L_1=5000 m and L_2=3000 m. For remaining parameters see Table 1. Equilibrium flow curves for inlets 1 (red) and 2 (green). (For interpretation of the references to colour in this figure legend, the reader is referred to the web version of this article.)

vectors $d\vec{A}_i/dt$, calculated from Eqs. (5) and (9), results in the flow diagram depicted in Fig. 5. From this flow diagram and the zoomed -in parts around the two equilibriums ($A_{1,eq1}$, $A_{2,eq1}$) and ($A_{1,eq2}$, $A_{2,eq2}$) (Fig. 6a and b), it follows that both equilibriums are unstable. Calculations with combinations of different inlet lengths, L_1 and L_2 and friction values F_1 and F_2 showed similar flow diagrams and no stable equilibriums (Borsje, 2003; Brouwer 2006). As an example the flow diagram with L_1=5000 m and L_2=3000 m is presented in Fig. 7. The remaining parameters are the same as those listed in Table 1. Because none of the numerical examples showed a stable equilibrium this supports the earlier conclusion in Van de Kreeke (1990) that, when assuming a uniformly fluctuating water level in the basin, there is no combination of inlet cross-sectional areas for which both inlets are stable.

3.2. Two-inlet bay system with topographic high

3.2.1. Governing equations

For the schematization of the two-inlet bay system with topographic high reference is made to Fig. 2b. Prismatic inlet channels with a triangular cross-section are assumed. The topographic high is introduced as a barrier with a uniform elevation and extending across the bay. The equations governing the water motion are the continuity equations for the two basins,

$$A_{b_1}\frac{d\eta_{b_1}}{dt} = u_1A_1 - u_3A_3 \tag{18}$$

and

$$A_{b_2}\frac{d\eta_{b_2}}{dt} = u_2A_2 + u_3A_3 \tag{19}$$

together with the equations of motion for the two inlets,

$$\frac{R_1}{F_1}\frac{du_1}{dt} + |u_1|u_1 = K_1(\eta_1 - \eta_{b_1}) \tag{20}$$

and

$$\frac{R_2}{F_2}\frac{du_2}{dt} + |u_2|u_2 = K_2(\eta_2 - \eta_{b_2}) \tag{21}$$

The ocean tides η_1 and η_2 are taken the same and are given by Eq. (13).

The equation of motion for the topographic high is

$$\frac{R_3}{F_3}\frac{du_3}{dt} + |u_3|u_3 = K_3(\eta_{b_1} - \eta_{b_2}) \tag{22}$$

As before subscripts 1 and 2 refer to inlets 1 and 2. The subscript 3 refers to the topographic high. In particular A_3 is the

Table 2
Parameter values used in calculating Figs. 8, 9 and 10

$L_1=L_2$=5000 m L_3=1000 m
$F_1=F_2=F_3$=0.004
W=25,000 m
$\gamma_1=\gamma_2$=0.065
$A_{b1}=A_{b2}=7\cdot10^8$ m^2
$\hat{u}_{eq}$=1.03 m/s
$\eta_1=\eta_2$=0.75 cos σt

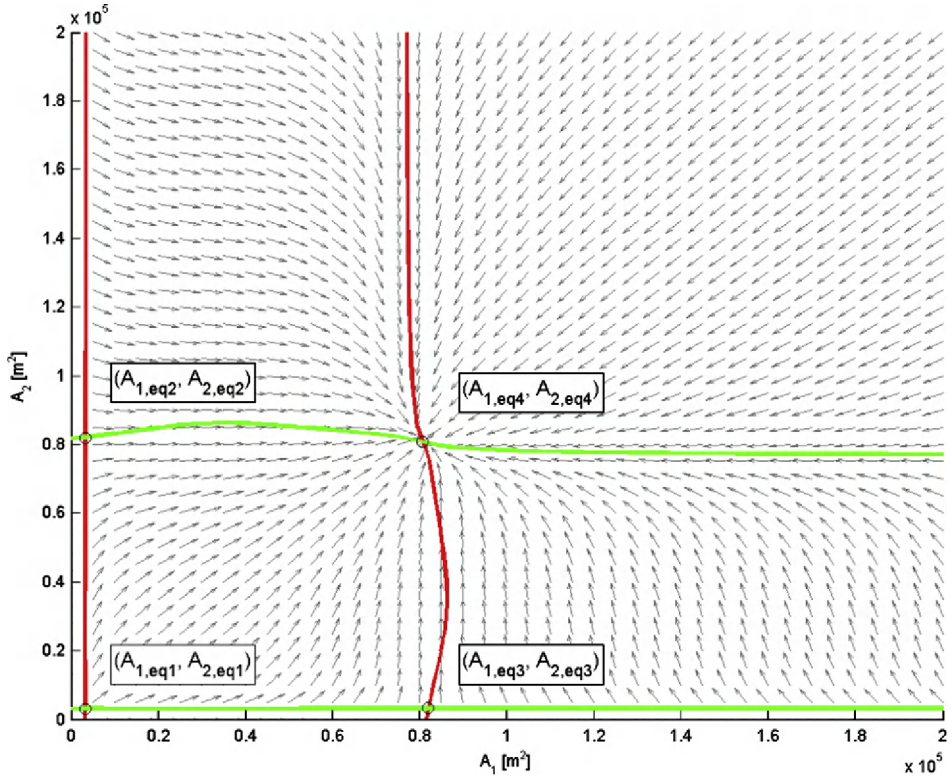

Fig. 8. Flow diagram for a two-inlet bay system with topographic high. For parameter values see Table 2. $A_3 = 10{,}000$ m^2. Equilibrium flow curves for inlets 1 (red) and 2 (green). (For interpretation of the references to colour in this figure legend, the reader is referred to the web version of this article.)

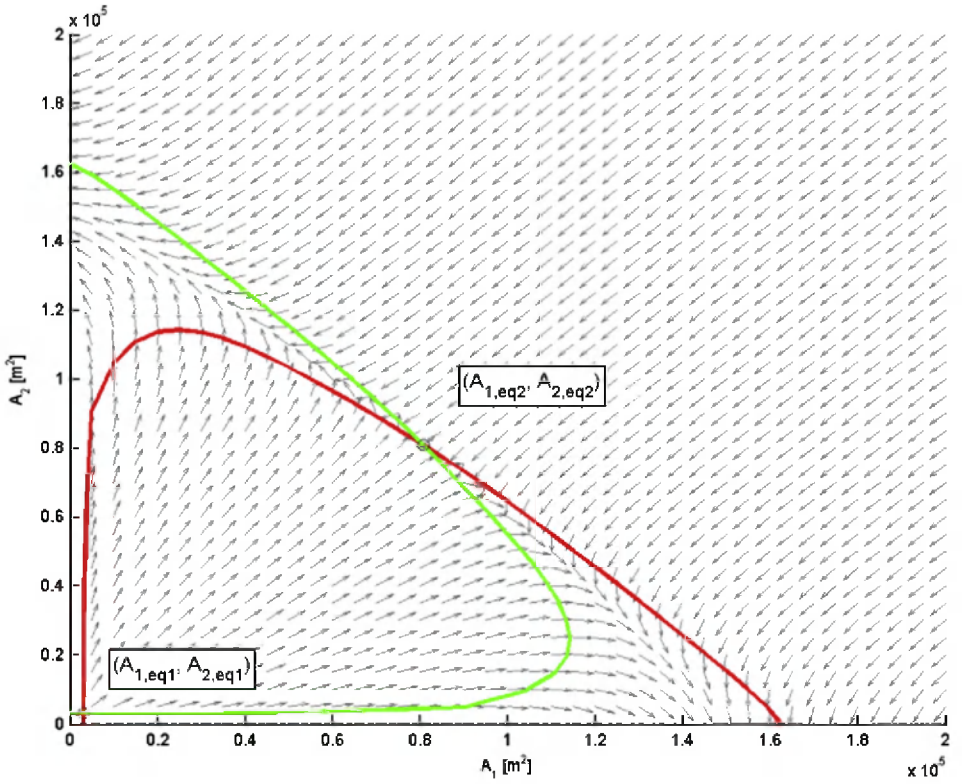

Fig. 9. Flow diagram for a two-inlet bay system with topographic high. For parameter values see Table 2. $A_3 = 100{,}000$ m^2. Equilibrium flow curves for inlets 1 (red) and 2 (green). (For interpretation of the references to colour in this figure legend, the reader is referred to the web version of this article.)

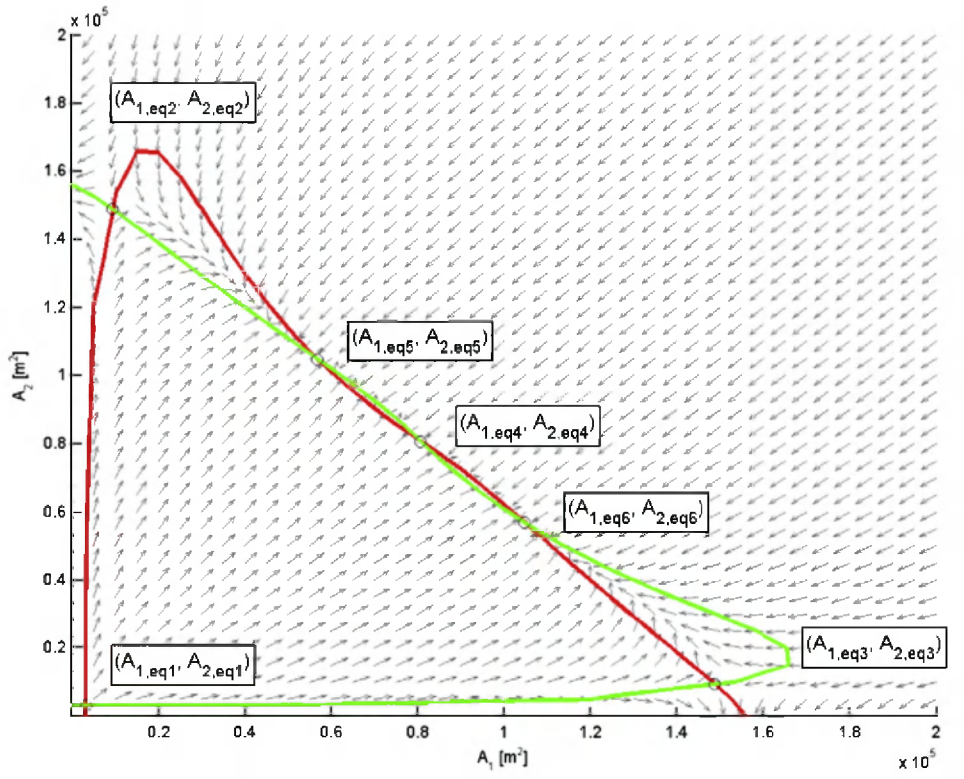

Fig. 10. Flow diagram for a two-inlet bay system with topographic high. For parameter values see Table 2. A_3 = 60,000 m^2. Equilibrium flow curves for inlets 1 (red) and 2 (green). (For interpretation of the references to colour in this figure legend, the reader is referred to the web version of this article.)

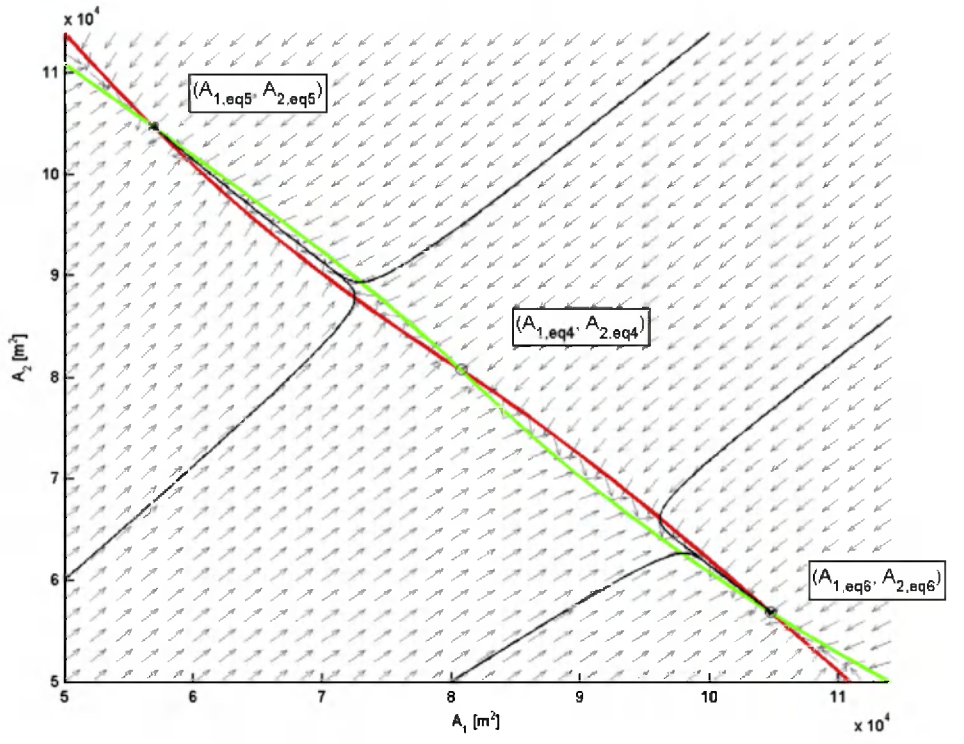

Fig. 11. Flow diagram for a two-inlet bay system with topographic high. Close-up of flow diagram in the vicinity of the equilibriums in Fig. 10. Black lines represent stream lines. Equilibrium flow curves for inlets 1 (red) and 2 (green). (For interpretation of the references to colour in this figure legend, the reader is referred to the web version of this article.)

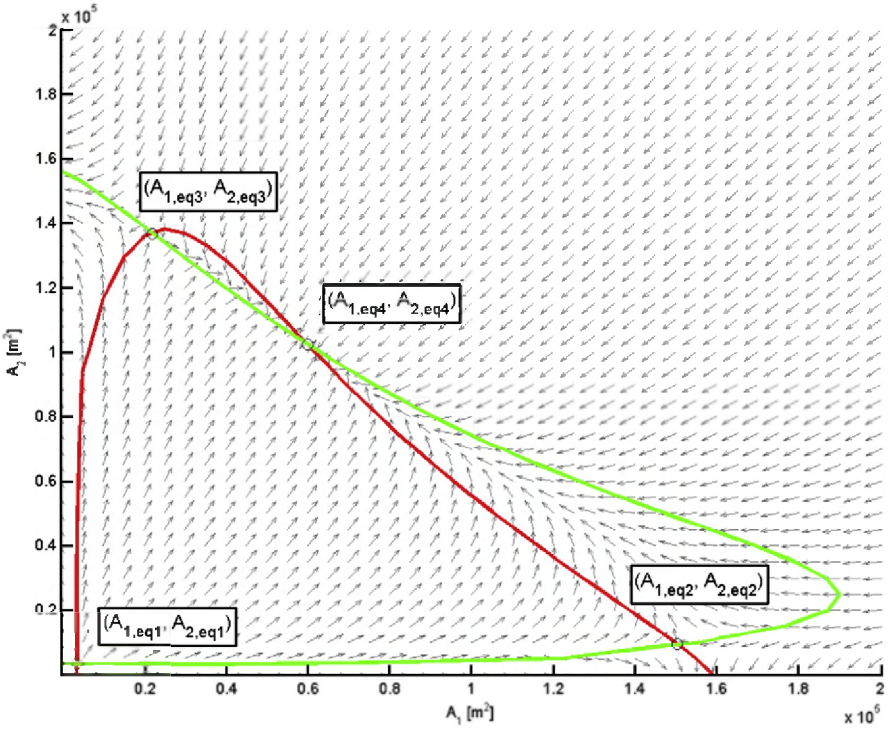

Fig. 12. Flow diagram for a two-inlet system with topographic high. $L_1=6000$ m and $L_2=5000$ m. For remaining parameters see Table 2. Equilibrium flow curves for inlets 1 (red) and 2 (green). (For interpretation of the references to colour in this figure legend, the reader is referred to the web version of this article.)

wetted cross-section over the topographic high. The repletion coefficients K_1 and K_2 are defined by Eq. (14). The repletion coefficient for the topographic high is

$$K_3 = \frac{gA_3}{F_3 L_3 W} \tag{23}$$

where L_3 is the cross-barrier width, W is the length of the barrier and F_3 is a dimensionless friction factor. When omitting the inertia term, Eq. (22) reduces to the equation describing steady flow over a weir.

3.2.2. Results

In the calculations emphasis has been on the effect of the wetted cross-section over the topographic high, A_3, on the number of equilibriums and their stability. Values used in the calculations are A_3 is 10,000 m^2, 60,000 m^2 and 100,000 m^2. For the remaining parameter values reference is made to Table 2. Cross-sections of the inlet channel are triangular with slopes that make a $1°$ angle with the horizontal. For the smallest opening the flow diagram is presented in Fig. 8. There are four equilibriums, only one of these, ($A_{1,eq4}$, $A_{2,eq4}$), is stable. Note that when the cross-section of the opening goes to zero, the equilibrium flow curves for inlets 1 and 2 reduce to two sets of lines that are parallel to respectively the A_2 and the A_1 axis. For the largest opening the flow diagram is presented in Fig. 9. There are two equilibriums that are both unstable. For the flow diagram of the intermediate opening see Fig. 10. There are six equilibriums, two of these, ($A_{1,eq5}$, $A_{2,eq5}$) and ($A_{1,eq6}$, $A_{2,eq6}$), are stable. To aid in the interpretation, a detailed flow diagram covering the region with the equilibriums ($A_{1,eq4}$, $A_{2,eq4}$), ($A_{1,eq5}$, $A_{2,eq5}$) and ($A_{1,eq6}$, $A_{2,eq6}$) in Fig. 10 is presented in Fig. 11.

The foregoing suggests that depending on the size of the wetted cross-section over the topographic high there can be one or more stable equilibriums. To further investigate the case of multiple stable equilibriums, calculations were carried out for $A_3=60{,}000$ m^2 and varying lengths of inlet 1. The remaining parameter values are those listed in Table 2. Instead of six equilibriums when taking $L_1=L_2$, in these calculations the number of

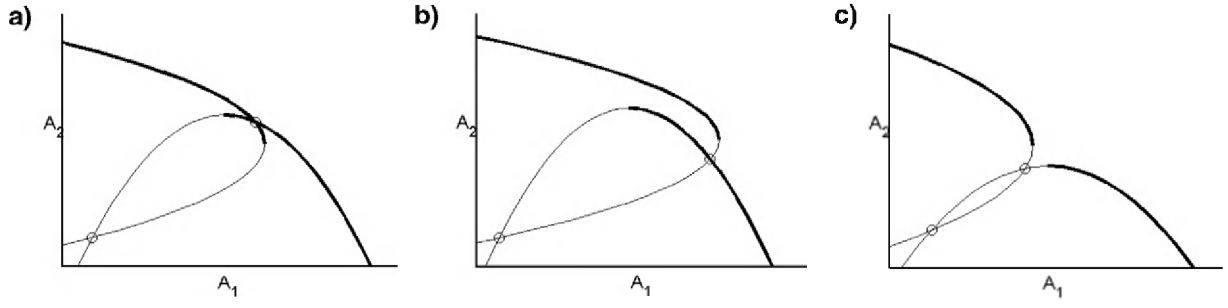

Fig. 13. Possible configurations of equilibrium flow curves for a two-inlet bay system without topographic high.

equilibriums is reduced to four with only one being stable. An example with $L_1=6000$ m and $L_2=5000$ m is shown in Fig. 12.

4. Discussion

For the two-inlet bay system without topographic high and identical sea surface elevations, the conclusion from the numerical experiments (Section 3.1.2) is that there will be at best two equilibriums neither of which is stable. This agrees with earlier conclusions in Van de Kreeke (1990). In the study presented in that paper Eqs. (11) and (12), are simplified by neglecting the inertia terms and linearizing the friction terms. With these simplifications two equations for the equilibrium cross-sectional area (A_{eq1}, A_{eq2}) are derived. It is shown that these equations have two sets of real roots. These two sets of real roots correspond to the two intersections of the equilibrium flow curves. There being two intersections limits the configuration of these curves to those presented in Fig. 13. From visual inspection of these curves, and keeping in mind that A_1 increases for $\hat{u}_{c_1}>\hat{u}_{eq}$and decreases for $\hat{u}_{c_1}<\hat{u}_{eq}$ and similar for A_2, it follows that neither of these equilibriums can be stable. For ease of reference the derivation in Van de Kreeke (1990) is summarized in Appendix A.

For two-inlet bay systems that include a topographic high and are forced by the same prescribed sea surface elevation off the inlets, results of numerical computations suggest that there can be more than two equilibriums some of which are stable. The exact number of equilibriums and their stability mode, in addition to the length and friction factor of the inlet channels, strongly depends on the wetted cross-section over the topographic high. For a relatively small cross-section the inlet-bay system behaves as two separate single-inlet bay systems. In that case the two sub-basins act independently and the equilibrium flow curve for each inlet degenerates to two parallel lines. There are four equilibriums only one of which is stable. For a large wetted cross-section the inlet bay system approaches that of the two-inlet bay system without topographic high. There are at best two equilibriums that both are unstable. For the intermediate wetted cross-section the results become more complex. Depending on the length and friction factor of the inlet channels, there can be as many as six equilibriums two of which are stable. The exact causes and conditions that determine the number of stable equilibriums in case of an intermediate size wetted cross-section are not clear and are the subject of an ongoing study. It follows that topographic highs can play an important role in the stability of two-inlet bay systems. This was also recognized by Tambroni and Seminara (2006) in their study on the stability of the inlets connecting the Venice Lagoon to the Adriatic Sea. However, they then proceed in evaluating the stability of the inlets by assuming a uniformly fluctuating lagoon water level, essentially eliminating the effects of the topographic highs on the stability of the inlets.

A limitation of the present study is the assumption of the same ocean tides prescribed for both inlets at the seaward side. In nature this is not always the case. For example, the tides off the inlets Marsdiep Inlet and Vlie Inlet (Fig. 1) differ significantly both in amplitude and phase. The sensitivities of the model results to prescribed amplitude and phase differences are presently under investigation.

5. Conclusions

The equilibrium and stability of two-inlet bay systems with and without a topographic high in the bay are investigated using the results of numerical experiments. A major assumption in describing the hydrodynamics of the water motion for the two-inlet bay system without a topographic high is that the bay level as a whole fluctuates uniformly. Numerical experiments carried out for different bay surface area and inlet characteristics show at best two combinations of cross-sectional areas for which there is equilibrium. Using flow diagrams it is shown that both equilibriums are unstable. This is in agreement with earlier results of analytical studies in which it was shown that where two inlets connect the same bay to the ocean ultimately only one inlet will remain open and the other one will close.

The suggestion in the Introduction that a topographic high dividing the bay in two basins plays a role in the stability of the inlets is confirmed by the numerical experiments. In the presence of the topographic high the water level in the sub-basins rather than in the bay as a whole fluctuates uniformly. The numerical results suggest that for small cross-sectional areas over the topographic highs there is one set of stable equilibriums. In that case the two-inlet bay system approaches that of two single-inlet bay systems. For large wetted cross-sections there is no stable equilibrium; the system reduces to that of a two-inlet bay system without topographic high. In the transition region between small and large wetted cross-sections there can be as many as two stable equilibriums.

The analysis in this paper is restricted to inlet systems whereby the ocean tides off the inlets are the same. The effect on the stability of different ocean tides as well as the cause and conditions for which stable equilibriums and in particular stable multiple equilibriums occur is part of an ongoing study.

Appendix A. An approximate analytical solution for the number of equilibriums in case of a two-inlet bay system without a topographic high

To arrive at an analytical solution Eqs. (11) and (12) in the main text are simplified by neglecting the inertia term and linearizing the friction term. This results in the following set of equations:

$$A_b\frac{d\eta_b}{dt}=u_1A_1+u_2A_2 \tag{A1}$$

$$\frac{8}{3\pi}\hat{u}_1u_1=K_1(\eta_0-\eta_b) \tag{A2}$$

$$\frac{8}{3\pi}\hat{u}_2u_2=K_2(\eta_0-\eta_b) \tag{A3}$$

Where K_1 and K_2 are defined by Eq. (13) in the main text. The open boundary condition is:

$$\eta_0=\hat{\eta}_0e^{i\sigma t} \tag{A4}$$

Eqs. (A1)–(A3) constitute a set of three equations with unknowns η_b, u_1 and u_2. Eliminating η_b by differentiating

Eqs. (A2) and (A3) with respect to t results in two equations in u_1 and u_2. Inspection of Eqs. (A2) and (A3) shows that the phase of u_1 and u_2 is the same. Therefore a suitable trial solution is

$$u_1 = \hat{u}_1 e^{i(\sigma t-\alpha)} \quad u_2 = \hat{u}_2 e^{i(\sigma t-\alpha)} \tag{A5}$$

Substituting the trial solution and separating real and imaginary parts leads to the following four equations.

$$\frac{8}{3\pi}\hat{u}_1^2\sigma\cos\alpha - \frac{K_1}{A_b}(\hat{u}_1A_1 + \hat{u}_2A_2)\sin\alpha = K_1\hat{\eta}_0\sigma \tag{A6}$$

$$\frac{8}{3\pi}\hat{u}_1^2\sigma\sin\alpha + \frac{K_1}{A_b}(\hat{u}_1A_1 + \hat{u}_2A_2)\cos\alpha = 0 \tag{A7}$$

$$\frac{8}{3\pi}\hat{u}_2^2\sigma\cos\alpha - \frac{K_2}{A_b}(\hat{u}_1A_1 + \hat{u}_2A_2)\sin\alpha = K_2\hat{\eta}_0\sigma \tag{A8}$$

$$\frac{8}{3\pi}\hat{u}_2^2\sigma\sin\alpha + \frac{K_2}{A_b}(\hat{u}_1A_1 + \hat{u}_2A_2)\cos\alpha = 0 \tag{A9}$$

Squaring Eqs. (A6) and (A7) and adding results in the following equation for the velocity amplitudes

$$\left(\frac{\frac{8}{3\pi}A_b\sigma}{K_1}\right)^2 \hat{u}_1^4 = (A_b\sigma\hat{\eta}_0)^2 - (\hat{u}_1A_1 + \hat{u}_2A_2)^2 \tag{A10}$$

Squaring Eqs. (A8) and (A9) results in a similar equation

$$\left(\frac{\frac{8}{3\pi}A_b\sigma}{K_2}\right)^2 \hat{u}_2^4 = (A_b\sigma\hat{\eta}_0)^2 - (\hat{u}_1A_1 + \hat{u}_2A_2)^2 \tag{A11}$$

It follows from Eqs. (A10) and (A11) and making use of the expression for K_1 and K_2, Eq. (16) in the main text,

$$\frac{A_1}{A_2} = \left(\frac{c_2}{c_1}\right)^2 \left(\frac{\hat{u}_1}{\hat{u}_2}\right)^4 \tag{A12}$$

Taking $\hat{u}_1 = \hat{u}_2 = \hat{u}_{\mathrm{eq}}$ in Eqs. (A10) and (A12) results in the two equations for the equilibrium cross-sectional areas A_{eq1} and A_{eq2}.

$$\left(\frac{\frac{8}{3\pi}A_b\sigma}{c_1}\right)^2 \hat{u}_{eq}^4 = (A_b\sigma\hat{\eta}_0)^2 A_{\mathrm{eq}_1} - A_{\mathrm{eq}_1}^3 \hat{u}_{\mathrm{eq}}^2 \left[1 + \left(\frac{c_2}{c_1}\right)^2\right]^2 \tag{A13}$$

$$\frac{A_{\mathrm{eq}_1}}{A_{\mathrm{eq}_2}} = \left(\frac{c_2}{c_1}\right)^2 \tag{A14}$$

It can be shown that one root of Eq. (A13) is always negative. The other two roots are positive provided

$$A_b\sigma\hat{\eta}_0^3 > 3\sqrt{\frac{3}{2}}\left(\frac{8}{3\pi}\right)^2 \left(\frac{1}{c_1^2} + \frac{1}{c_2^2}\right) \tag{A15}$$

It follows from the foregoing that there are at best two combinations of cross-sectional areas for which both inlets are in equilibrium.

References

Borsje, C.S., 2003. Cross-sectional stability of a two-inlet bay system. M.Sc theses, Department of Civil Engineering, Delft University of Technology, p. 60.

Brouwer, R.L., 2006. Equilibrium and stability of a double inlet system. M.Sc theses Department of Civil Engineering, Delft University of Technology, p. 81.

Brown, E.I., 1928. Inlets on Sandy Coasts. Proc. Amer. Society of Civil Engineers 505–553.

Bruun, P., Gerritsen, F.F., 1960. Stability of coastal inlets. North Holland publishing company, Amsterdam. 123.

DiLorenzo, J.L., 1988. The overtide and filtering response of small inlet/bay systems. In: Aubrey, D.G., Weishar, L. (Eds.), Hydrodynamics and Sediment Dynamics of Tidal Inlets, pp. 24–53.

Escoffier, F.F., 1940. The stability of tidal inlets. Shore and Beach 8 (4), 111–114.

Jain, M., Mehta, A.J., van de Kreeke, J., Dombrowsky, M.R., 2004. Observations on the stability of St. Andrew Bay Inlets in Florida. Journal of Coastal Research 20 (3), 913–919.

Jarrett, J.T., 1976. Tidal prism–inlet area relationships. Giti Report 3. Coastal Engineering Research Center. U.S. Army Corps of Engineers. 31.

Keulegan, G.H., 1951. Third progress report on tidal flow in entrances: water level fluctuations of basins in communication with seas. Report No 1146, National Bureau of Standards, Washington, DC. 28.

Kraus, N.C., 1998. Inlet cross-sectional area calculated by process-based model. Proceedings 26th International Conference on Coastal Engineering, vol. 3, pp. 3265–3278.

Louters, T., Gerritsen, F., 1994. The Riddle of the Sands; a tidal system's answer to a rising sea level. National Institute for Coastal and Marine Management. Report RIKZ-94.040, p. 69.

Mehta, A.J., Ozsoy, E., 1978. Inlet Hydraulics. In: Bruun, P. (Ed.), Stability of Tidal Inlets. Elsevier Scientific Publishing Company, p. 510.

O'Brien, M.P., 1931. Estuary Tidal Prism Related to Entrance Areas. Civil Engineering 1 (No. 8), 738.

O'Brien, M.P., Dean, R.G., 1972. Hydraulics and sedimentary stability of coastal inlets. Proceedings 13th International Conference on Coastal Engineering vol. 2, 761–780.

Salles, P., Voulgaris, G., Aubrey, D.G., 2005. Contribution of non-linear mechanisms in the persistence of multiple inlet systems. Estuarine Coastal and Shelf Science 65, 475–491.

Suprijo, T., Mano, A., 2004. Dimensionless parameters to describe topographical equilibrium of coastal inlets. Proceedings International Conference on Coastal Engineering 3, 2531–2543.

Tambroni, N., Seminara, G., 2006. Are inlets responsible for the morphological degradation of Venice Lagoon? J. Geophys Res. 111, F03013. doi:10.1029/2005JF000334.

Van de Kreeke, J., 1967. Water level fluctuations and flow in tidal inlets. Journal of the Waterways, Harbors and Coastal Engineering Division, American Society of Civil Engineers 93 (WW4), 97–106.

Van de Kreeke, J., 1990. Can multiple inlets be stable? Estuarine, Coastal and Shelf Science 30, 261–273.

Van de Kreeke, J., 1998. Adaptation of the Frisian Inlet to a Reduction in Basin Area with Special Reference to the Cross-sectional Area of the Inlet Channel. In: Dronkers, J., Scheffers, M.B.A.M. (Eds.), Physics of Estuaries and Coastal Seas. Proceedings 8th International Biennial Conference Physics of Estuaries and Coastal Seas (PECS), pp. 355–362.

Van de Kreeke, J., 2004. Equilibrium and stability of tidal inlets; application to the Frisian Inlet before and after basin reduction. Coastal Engineering 51, 337–350.

Walton Jr., T.L., Escoffier, F.F., 1981. Linearized solution to inlet equation with inertia. Journal Waterway, Port, Coastal and Ocean Division, ASCE, WW3 191–195.

Walton Jr., T.L., 2004. Escoffier curves and inlet stability. Journal of Waterway, Harbor, Coastal and Ocean Engineering 130 (1), 54–57 ASCE.